JOURNAL OF VIROLOGY, Nov. 2004, p. 12557–12565 Vol. 78, No. 22
0022-538X/04/$08.00+0 DOI: 10.1128/JVI.78.22.12557–12565.2004


# Generation of Synthetic Severe Acute Respiratory Syndrome Coronavirus Pseudoparticles: Implications for Assembly and Vaccine Production

Yue Huang, Zhi-yong Yang, Wing-pui Kong, and Gary J. Nabel*

*Vaccine Research Center, National Institute of Allergy and Infectious Diseases, National Institutes of Health, Bethesda, Maryland*

Received 4 March 2004/Accepted 29 June 2004

**The recently emerged severe acute respiratory syndrome coronavirus (SARS-CoV) contains four structural genes, two replicase-transcriptase open reading frames, and more than five potential genes of unknown function. Despite this relative simplicity, the molecular regulation of SARS-CoV replication and assembly is not understood. Here, we report that two viral genes, encoding the SARS-CoV membrane (M) and nucleocapsid (N) proteins, are necessary and sufficient for formation of virus-like particles. Expression vectors encoding these two proteins were synthesized by using preferred human codons. When M and N expression plasmids were cotransfected into human 293 renal epithelial cells, pseudoparticles formed readily. The addition of a third gene, encoding the spike (S) glycoprotein, facilitated budding of particles that contained a corona-like halo resembling SARS-CoV when examined by transmission electron microscopy, with a buoyant density characteristic of coronaviruses. Specific biochemical interactions of these proteins were also shown in vitro. The S, M, and N proteins of the SARS-CoV are, therefore, necessary and sufficient for pseudovirus assembly. These findings advance the understanding of the morphogenesis of SARS-CoV and enable the generation of safe, conformational mimetics of the SARS virus that may facilitate the development of vaccines and antiviral drugs.**

The severe acute respiratory syndrome coronavirus (SARS-CoV) is the causative agent of recently recognized SARS (9, 18). This virus, an enveloped, positive-strand RNA coronavirus, displays a host range different from previous family members, which may contribute, in part, to its pathogenicity. Approximately 31 kb in length, the viral genome encodes structural, replicative, and regulatory proteins that control viral attachment, entry, gene expression, RNA replication, assembly, and pathogenicity. This viral genome is highly conserved, although mutations have already been defined that may contribute to genetic diversity (14, 31). Coronaviruses can replicate in the respiratory and/or gastrointestinal tract (15, 20). The SARS-CoV has apparently evolved the capacity to replicate in both sites, though its specific target cells in vivo have not been fully defined.

Coronaviruses typically contain three or four structural proteins. The membrane (M) glycoprotein is among the most abundant, spanning the membrane bilayer three times, with a long COOH-terminal cytoplasmic domain inside the virion and a short $NH_2$-terminal domain outside (15, 22, 27). The spike (S) glycoprotein represents a type I membrane glycoprotein that gives rise to peplomers which mediate binding and attachment to target cells. The nucleocapsid (N) protein is an internal phosphoprotein of 50 to 60 kDa that interacts with viral genomic RNA to form the viral core. The small envelope (E) protein has been detected as a minor structural component in avian infectious bronchitis virus (IBV), transmissible gastroenteritis virus (TGEV), and mouse hepatitis virus (MHV) particles (32).

Despite the rapid isolation and identification of the SARS-CoV, determination of its genetic sequence, and cloning of its receptor ACE2 (18, 21, 26, 28, 30), the molecules required for SARS-CoV assembly remain unknown. Coronaviruses are typically described as budding enveloped viruses with corona-like S proteins protruding from the surface. These positive-stranded RNA viruses are approximately 100 nm in size and derive their envelopes from the host cell, presumably the membrane of the endoplasmic reticulum or Golgi apparatus (15, 20). Previous evidence indicates that the E and M proteins are instrumental in this process. Studies have suggested, for example, that MHV E and M proteins are sufficient to produce membrane-bound particles very similar to virions in size and shape (5, 6, 34) though they differ in sequence from the SARS E and M proteins. Similarly, the roles of these structural genes in the assembly of other coronaviruses, such as IBV, also have been defined (4). Because SARS-CoV has a limited number of open reading frames whose functions have not been defined, we attempted to analyze the role of specific genes in virus assembly by transfecting synthetic, codon-modified S, M, N, and E expression vectors into mammalian cells.

## MATERIALS AND METHODS

**Development of synthetic SARS-CoV expression vectors.** The methods used to create the synthetic SARS-CoV expression vectors have been previously described (2, 16). Briefly, the protein sequences of S, N, M, and E from the SARS-CoV Urbani strain (GenBank accession number AY278741) (30) were reverse translated by a GCG Package (Genetic Computer Group, Inc., Madison, Wis.), using the codons expected for human cells. Oligonucleotides covering these four genes were purchased from Sigma-Genosys Inc. Each of the oligonucleotides was 75 bases in length, with 25 nucleotides of overlap between segments. The codon-modified genes were assembled by PCR *PfuTurbo* Hotstart (Stratagene) high-fidelity DNA polymerase. The PCR conditions were optimized with a PCR optimization kit (Stratagene) on a gradient Robocycler (Stratagene). Full-length synthetic S, N, M, and E proteins were cloned into the XbaI and BamHI sites of the mammalian expression vector CMV/R derived from pNGVL-3 (25) and confirmed by DNA sequencing. Mutations of M were created by PCR with the following primers: CAGATATCGCCGCCACCATGCAGCTGCTGG

* Corresponding author. Mailing address: Vaccine Research Center, NIAID, National Institutes of Health, Bldg. 40, Room 4502, MSC 3005, 40 Convent Dr., Bethesda, MD 20982-3005. Phone: (301) 496-1852. Fax: (301) 480-0274. E-mail: gnabel@nih.gov.

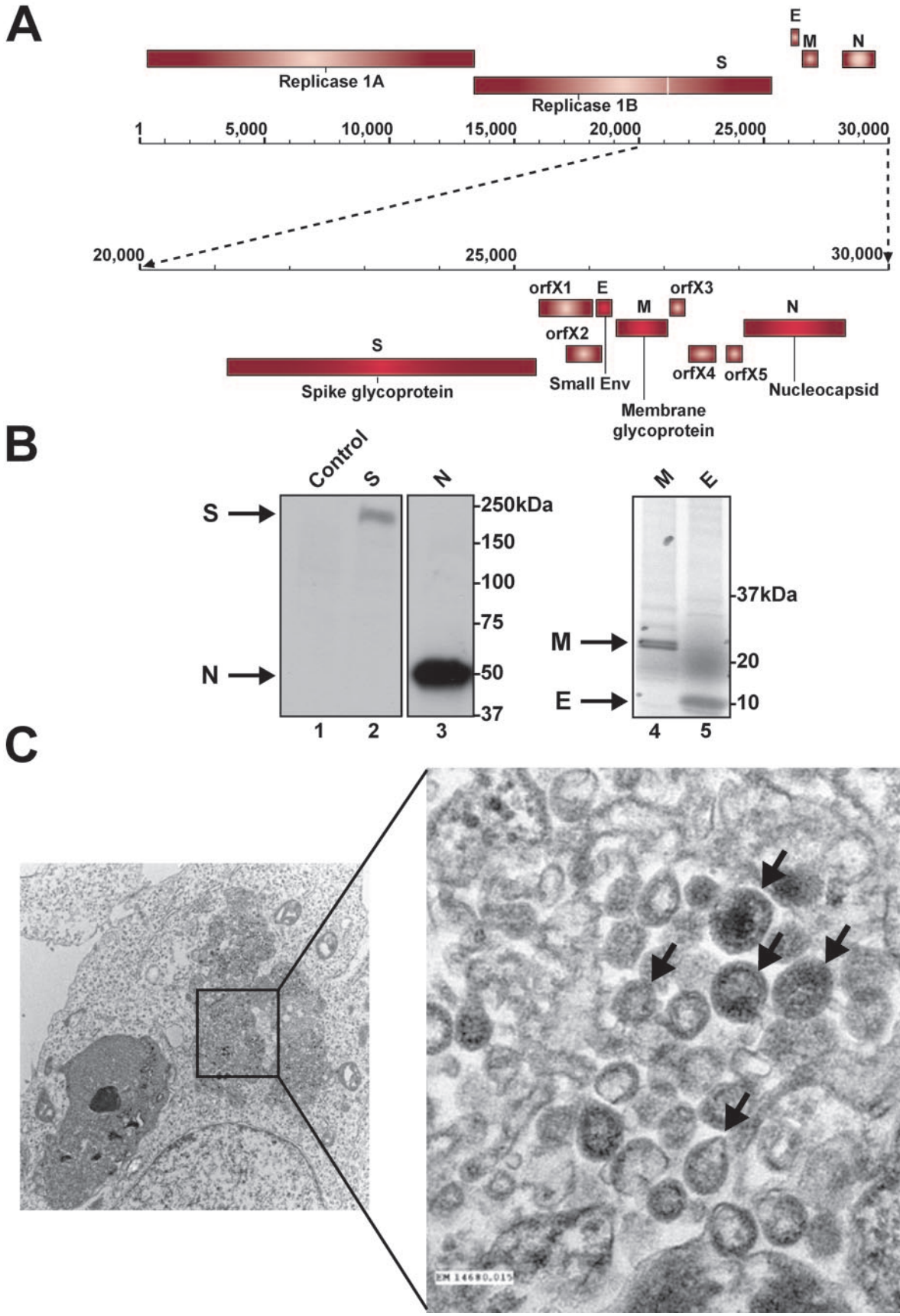
A
E
M
N
S
Replicase 1A
Replicase 1B
1
5,000
10,000
15,000
20,000
25,000
30,000
20,000
25,000
30,000
orfX1
E
orfX3
M
N
orfX2
S
orfX4
orfX5
Spike glycoprotein
Small Env
Membrane glycoprotein
Nucleocapsid
B
Control
S
N
M
E
S
N
250kDa
150
100
75
50
37
37kDa
20
10
1
2
3
4
5
C

AGCAGTGGAACCT and AGAGCGGCCGCTCACTGCACCAGCAGGGC GATGTTGTCGT for $M\Delta N_{12}$ (lacking the putative extracellular domain); CA GATATCGCCGCCACCATGGCCGACAACGGCACCATCACCG and AG AGCGGCCGCTCACTGCACCAGCAGGGCGATGTTGTCGT for MΔTM (lacking the transmembrane domains); and CAGATATCGCCGCCACCATGG CCGACAACGGCACCATCACCGT and GAGCGGCCGCTCACCTGAAGC TGGCCACGAAGTAGCTCAGCCA for MΔC (lacking the putative cytoplasmic domain). The PCR fragments containing the M mutations were digested with EcoRV-NotI and cloned into the same sites of CMV/R and pcDNA3.1(+). All the mutations and PCR fragments were confirmed by sequencing.

**Transient transfection and EM.** 293T cells were maintained in Dulbecco's modified Eagle medium (DMEM; GIBCO-BRL), supplemented with 10% fetal bovine serum. Plasmid DNAs were purified by using double cesium chloride sedimentation gradients. Approximately $3 \times 10^6$ 293T cells were placed in a 10-cm dish 1 day before transfection. Three micrograms of each plasmid (each containing one of the SARS-CoV genes) was mixed and used to transfect 293T cells by the calcium phosphate method (3). The vector backbone was used as filler DNA to maintain the same amount of DNA in each transfection. At 63 h after transfection, the cells were lifted from plates by resuspension with DMEM and then pelleted in a 15-ml conical tube by centrifugation at 1,000 rpm in a Sorvall desktop centrifuge. The supernatant was removed, and a 10-fold volume of fixing solution was added (3% glutaraldehyde and 3% formaldehyde, cacodylate buffer [pH 7.3]) (Tousimis Research Corporation, Rockville, Md.). The specimens were mixed gently and analyzed in the electron microscopy (EM) core laboratory at the University of Michigan Health Center.

**Viral capsid production and buoyant density gradient analysis.** A total of $3 \times 10^6$ 293T cells were transfected with 3 μg each of pCMV/R-S, N, and M in a 10-cm tissue culture dish with DMEM. The cells were harvested after 3 days and freeze-thawed three times in phosphate-buffered saline. The cleared lysates were pelleted onto 50% of an OptiPrep (Iodixanol) medium (Invitrogen) at 20,000 rpm with a Sorvall Surespin 630 rotor, and the final concentration of OptiPrep was adjusted to 30%. A density gradient was formed by centrifugation at 75,000 rpm for 3.5 h with an NTI100 rotor, according to the manufacturer's instructions (Invitrogen). The collected fractions were weighted at 100 μl of each fraction and plotted with density by fractions. Twenty microliters of each fraction was separated on sodium dodecyl sulfate-polyacrylamide gel electrophoresis (SDS-PAGE) 4 to 15% acrylamide gels, transferred onto an Immobilon-P membrane, and blotted with human anti-SARS-CoV serum. Each lane of the Western blot represents and fits with one fraction of self-gradient OptiPrep containing the cell lysates.

**Western blotting and in vitro translation analysis.** Human anti-SARS-CoV serum samples were a gift from William Bellini of the Centers for Disease Control and Prevention. Western blotting was performed as previously described (12). The $^{35}$S-labeled proteins were in vitro translated individually from plasmid DNA by a TNT T7 Quick Coupled Transcription/Translation System from Promega. For the synthesis of M and E, 1 μl of canine pancreatic microsomal membranes (Promega) was added to the reactions.

**Immunoprecipitation.** The $^{35}$S-labeled proteins were in vitro translated individually from plasmid DNA by a TNT T7 Quick Coupled Transcription/Translation System from Promega, according to the user's manual. One microliter of canine pancreatic microsomal membrane (Promega) was added to improve the expression of the S, M, and E proteins. Ten microliters of [$^{35}$S]methionine-labeled M and mutant M proteins was mixed with 10 μl of His-tagged N protein translated with 1 mM methionine for N pull-down of M and M mutants and incubated with 1 μg of rabbit polyclonal anti-His antibody (Santa Cruz Biotechnology Inc., Santa Cruz, Calif.) at 4°C for 1 h. This product was immunoprecipitated with 500 μl of immunoprecipitation buffer containing 50 mM Tris-HCl (pH 7.4), 150 mM NaCl, 1% NP-40, and 1 mM dithiothreitol plus proteinase inhibitor cocktail for 1 h at 4°C. Ten microliters of protein G agarose (Invitrogen), washed three times, was added and incubated for 1 h. After being washed five times with the buffer described above, the pellets were boiled in SDS gel loading buffer and resolved by SDS-PAGE with autoradiography. For S immunoprecipitation of M, E, and N, 10 μl of [$^{35}$S]methionine-labeled N, M, and E or a negative control protein, human immunodeficiency virus (HIV) gp145, was mixed with 10 μl of S translated with 1 mM methionine and immunoprecipitated with 1 μg of human anti-SARS-CoV monoclonal antibody (a gift from Antonio Lanzavecchia) in 400 μl of buffer II (for membrane protein extraction) from a subcellular extraction kit (Calbiochem). After being washed three times with the immunoprecipitation buffer described above, the pellets were boiled in SDS gel loading buffer and resolved by SDS-PAGE with autoradiography. A mutant HIV envelope protein, B-clade gp145ΔCFI, with a transmembrane domain was also translated with 1 mM methionine (unlabeled) and used as a negative control immunoprecipitation with 1 μg of 2G12 antibody to HIV envelope, as described for S pull-down.

## RESULTS

To define the SARS-CoV genes essential for viral assembly, mammalian expression vectors encoding different viral genes were analyzed. These genes included the S, M, N, and E proteins (Fig. 1A) synthesized from the predicted amino acid sequence by reverse translation, with codon usage typical of human cells. The DNA sequence of each gene was confirmed, and expression was confirmed by Western blot analysis or in vitro transcription-translation (Fig. 1B). To evaluate the contribution of these gene products to viral assembly, the expression of the SARS-CoV S, M, N, and E genes was analyzed in different combinations in transfected 293 cells. Coexpression of all four gene products resulted in the assembly of electron-dense structures that resembled pseudoparticles of ~100 nm (Fig. 1C), characteristic of the SARS coronavirus. The absence of positive-stranded viral genomic RNA, protease, or the viral polymerase indicated that they were not essential for the formation of the SARS-CoV core particles, though the central lucency raised the possibility that RNA was taken up nonspecifically by the pseudoparticles (Fig. 1C, right panel).

To examine the minimum requirements for pseudoparticle formation, different combinations of these viral genes were analyzed systematically by cotransfection. Any combination of genes that expressed M and N, with or without S and/or E, was able to generate intracellular virus-like particles (VLPs), and the pseudoparticles did not form in the absence of the M and N proteins (Table 1 and Fig. 2). No single viral gene was able to support the formation of viral capsids within these cells. These structures were localized primarily to endosomal vesicles and were seen most prominently in juxtaposition to the nucleus (Fig. 3A), which is typical of many coronaviruses. They

FIG. 1. SARS-CoV gene organization and analysis of viral assembly by transmission EM. (A) Schematic representation of the SARS-CoV genome. The genes encoding viral proteins are drawn to scale. Bars denote the coding regions, and lines indicate the noncoding sequences. From 5′ to 3′, orf1, orf2, S, E, M, N, and unknown open reading frames (orf X1 to orf X6) are indicated. (B) Expression of S, M, N, and E gene products by in vitro transcription-translation and/or Western blot analysis. The synthetic gene products, S and N, prepared as described in Materials and Methods as mammalian expression vectors, were transfected into 293 cells and analyzed by Western blot analysis with convalescent human sera, kindly provided by William Bellini of the Centers for Disease Control (left). Because this antisera did not react with them, M and E were prepared first in plasmids under the control of the T7 polymerase promoter and transcribed and translated by using a rabbit reticulocyte lysate, followed by analysis with SDS-PAGE after labeling with [$^{35}$S]methionine (right). (C) Electron micrograph of SARS-CoV capsids in transfected 293T cells. Two micrograms of each of four plasmids coding for the S, M, N, and E proteins was used to cotransfect $3 \times 10^6$ 293T cells by the calcium phosphate method (a total of 8 μg of DNA per transfection). Transmission EM analysis was performed by using the method described in the note to Table 1 (magnification, ×7,000) (left). A high-power view (magnification, ×150,000) of the inset shows 293 cells cotransfected with four plasmids (2 μg each) encoding S, M, N, and E transfected as described above (right).

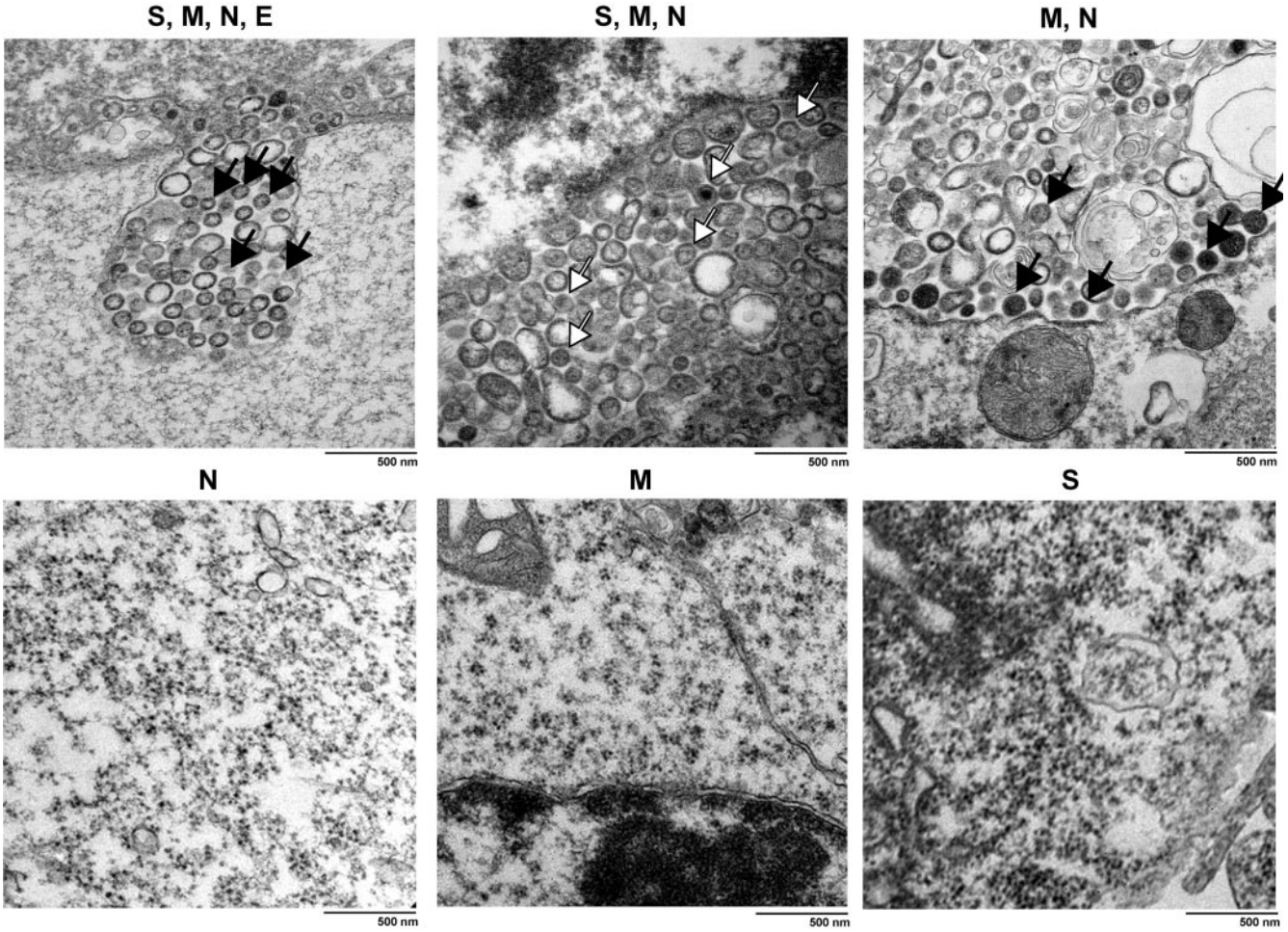


FIG. 2. Analysis by transmission EM of the contribution of different viral gene products to viral assembly. Nucleocapsid formation by cotransfection of the indicated combinations of expression vectors encoding the specified viral gene products. Transfections were performed as described in the legend of Fig. 1 (magnification, ×40,000).

appeared similar in size and morphology to replication-competent virus (18). Though cotransfection of the N and M proteins allowed detection of viral pseudoparticles intracellularly, no budding virus or corona-like structures were visible in these transfected cells. The addition of the S glycoprotein, however, allowed for budding and formation of a corona-like structure (Fig. 3B), indicating that S is likely to be important not only for viral fusion but also for maturation and egress from cells.

To characterize these synthetic SARS-CoV particles further, we performed buoyant density gradient sedimentation analysis. Because the capsid core was found in higher quantities within cells, lysates were prepared from transfected cells that were frozen and thawed three times. When fractions from a gradient of clarified cell lysates were analyzed by Western blotting with human immune serum, the peak of viral protein expression, composed primarily of N and S proteins (Fig. 4A), was detected at a density of 1.18 g/ml (Fig. 4B), comparable to the buoyant density described for other coronaviruses (24). The specificity of this gradient was further confirmed by transfection with N alone, which was distributed evenly across the gradient and did not show a buoyant density similar to the pseudoparticles (Fig. 4A).

To determine the specific domains required for SARS-CoV VLP assembly, deletion mutants of the M protein were prepared. A membrane-spanning structure was predicted by the SOSUI computer program (http://sosui.proteome.bio.tuat.ac.jp), and three recognizable domains were identified: an $NH_2$-terminal 12-amino-acid extracellular domain, a central region with three membrane spanning segments, and a COOH-terminal cytoplasmic domain (Fig. 5A). These domains also exist in IBV and MHV and are essential for viral assembly (5, 6, 10). Three mutants were therefore created with either a deletion of the putative extracellular domain ($M\Delta N_{12}$), excision of the transmembrane domains (MΔTM), or removal of the putative cytoplasmic domain (MΔC). In vitro transcription-translation showed that these mutants expressed proteins of the expected size (Fig. 5B). Coexpression of N with mutant M genes that lacked either the transmembrane or the cytoplasmic domain abolished its ability to form pseudoparticles (Fig. 5C). In contrast, deletion of the $NH_2$-terminal putative extracellular region had no effect on particle formation (Fig. 5C), indicating

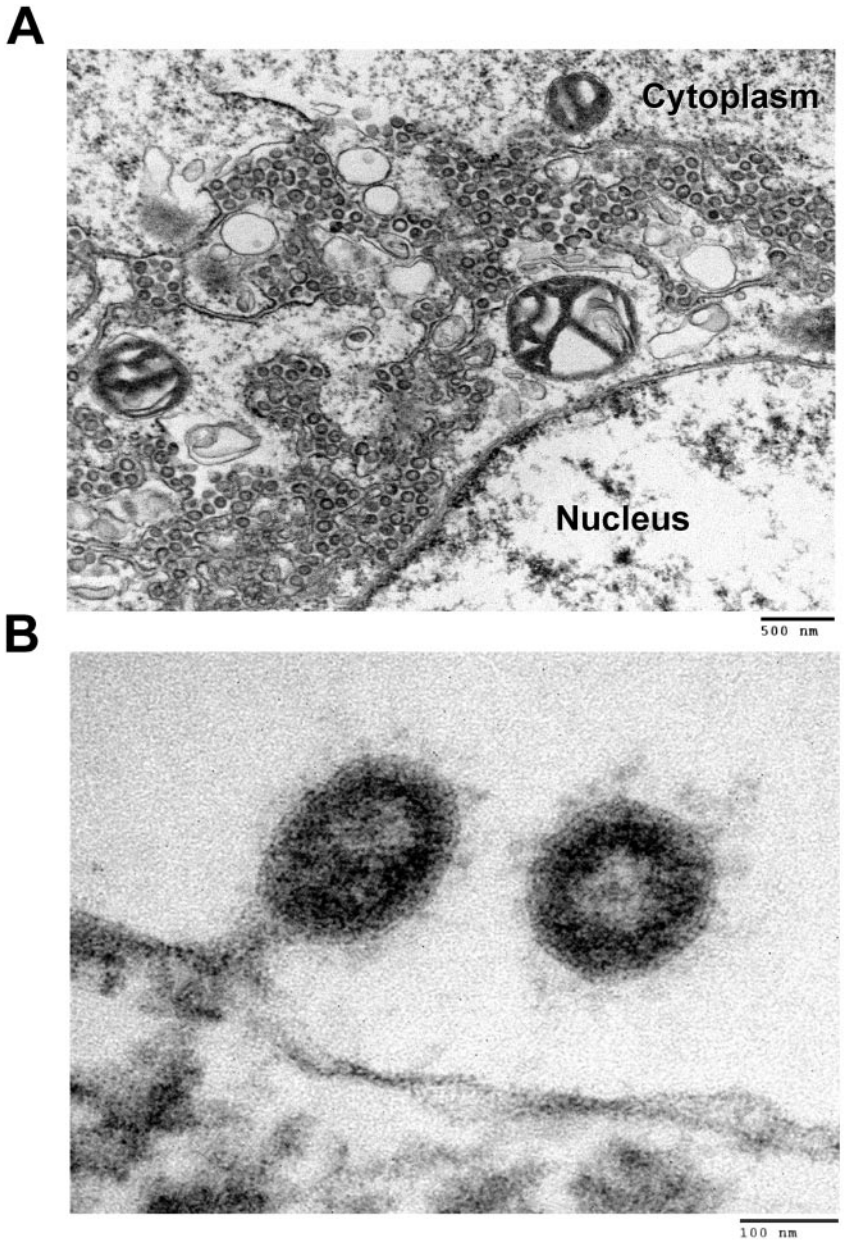


FIG. 3. Formation of coronavirus-like particle by inclusion of S glycoprotein expression vector. Electron micrograph of virus particles in 293T cells transfected, as described in the note to Table 1, with S, M, and N. High-power view of VLPs forming in the cytoplasm juxtaposed to the nuclear membrane (magnification, ×30,000) (A) and formation of a VLP with a corona-like structure emerging from an intracellular membrane (magnification, ×200,000) (B).

that both transmembrane and cytoplasmic domains of M are required for viral particle formation.

The interaction between these viral proteins was analyzed further to establish the biochemical basis for virus particle formation. The major structural proteins were synthesized by transcription with T7 RNA polymerase and translation with rabbit reticulocyte lysates in vitro, as were mutant forms of M (Fig. 5B and D). Canine pancreatic microsomal membranes were added to improve the expression of S, E, M, and the three M mutants and to model the membrane interactions. The full-length M protein was able to associate with the COOH-terminal His-tagged N protein when they were coincubated at 30°C for 30 min and were then pulled down with polyclonal anti-His antibody (Fig. 5B, lane 7). In fact, the soluble COOH-terminal region of M bound more avidly to N than to the full-length protein, suggesting that this interaction was specific and localized to the cytoplasmic domain of the protein (Fig. 5B, lane 9), which may be less well exposed during protein translation of the complete protein in vitro. In contrast, we were unable to detect an interaction of the S glycoprotein with N, though it did bind to M and E (Fig. 5D, lane 17 versus lanes 18 and 19). A control membrane-binding protein, gp145, did not bind to S, N, M, or E under the same conditions (Fig. 5D, lanes 16, 20, 21, and 22). Together, these findings suggest that M plays a

TABLE 1. Summary of SARS-CoV capsid formation after cotransfection of viral genes by scanning transmission EM[a]

| SARS-CoV genes | | | | Capsid formation |
|---|---|---|---|---|
| N | M | S | E | |
| + | + | + | + | + |
| + | + | + | − | + |
| + | + | − | + | + |
| + | + | − | − | + |
| + | − | + | + | − |
| + | − | + | − | − |
| + | − | − | + | − |
| + | − | − | − | − |
| − | + | + | + | − |
| − | + | + | − | − |
| − | + | − | + | − |
| − | − | + | + | − |
| − | + | − | − | − |
| − | − | + | − | − |
| − | − | − | + | − |
| − | − | − | − | − |

[a] A total of $3 \times 10^6$ 293T cells were transfected with plasmids containing the indicated genes as described in Materials and Methods. The specific viral genes and formation of intracellular viral capsids determined by scanning transmission EM are indicated.

pivotal role in nucleocapsid assembly through its ability to interact with N through its COOH-terminal cytoplasmic domain and with S through other regions (Fig. 6). It thus serves as a critical bridge between essential internal and external components of the virus.

## DISCUSSION

In this study, we find that the major structural genes for the SARS-CoV can be efficiently produced in transfected 293 cells and can support the production of synthetic SARS-CoV. The expression of two viral gene products, M and N, was necessary and sufficient for the formation of pseudoparticles. The additional expression of the S glycoprotein allowed the formation of budding particles with morphology typical of SARS and related coronaviruses. The finding that two viral genes were required for the formation of these viral particles contrasts with the assembly of retroviruses and lentiviruses, in which the expression of a single gene product, the Gag precursor polyprotein, is sufficient to form VLPs (8, 13, 16, 23, 33, 35). On the other hand, assembly of Ebola virus nucleocapsids requires three viral gene products, NP, VP35, and VP24, which perform complementary functions (17). Analogous to the process in

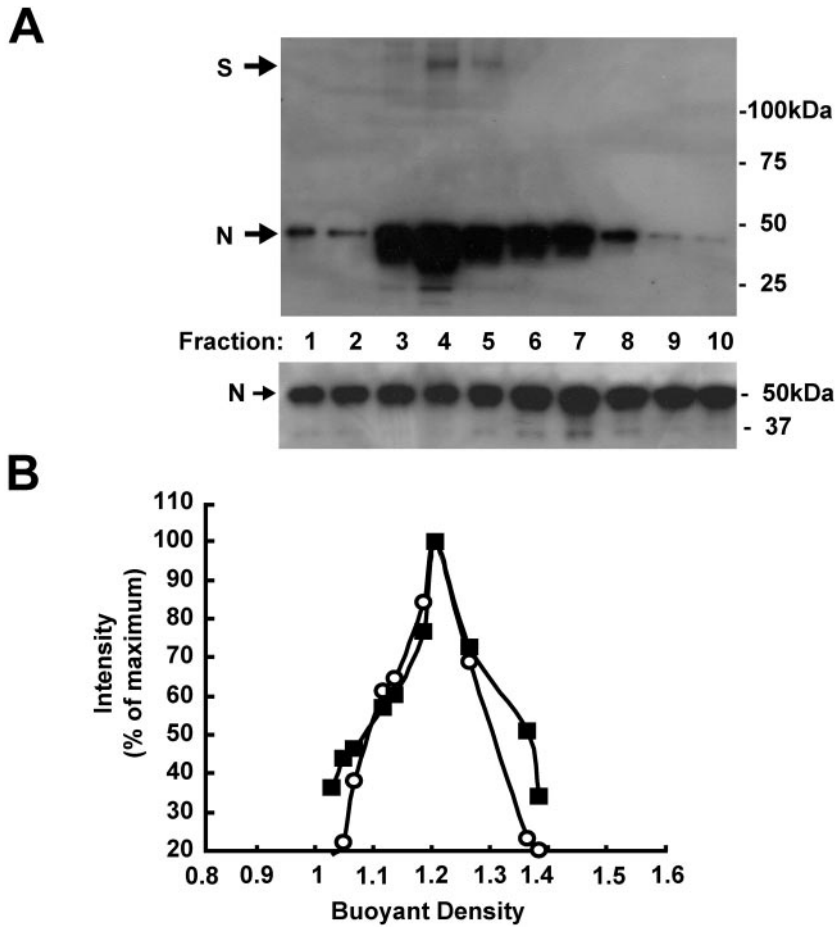


FIG. 4. Release of assembled capsids from transfected 293T cells and buoyant density gradient analysis. (A) Western blotting and gradient sedimentation analysis of assembled capsids from clarified cell lysates transfected with S, M, and N (top) or transfected N alone (bottom). Arrows indicate specific S or N proteins. (B) Quantitative morphometry of Western blot analysis of assembled capsids from panel A (top) indicates relative expression of S (filled squares) or N (open circles).

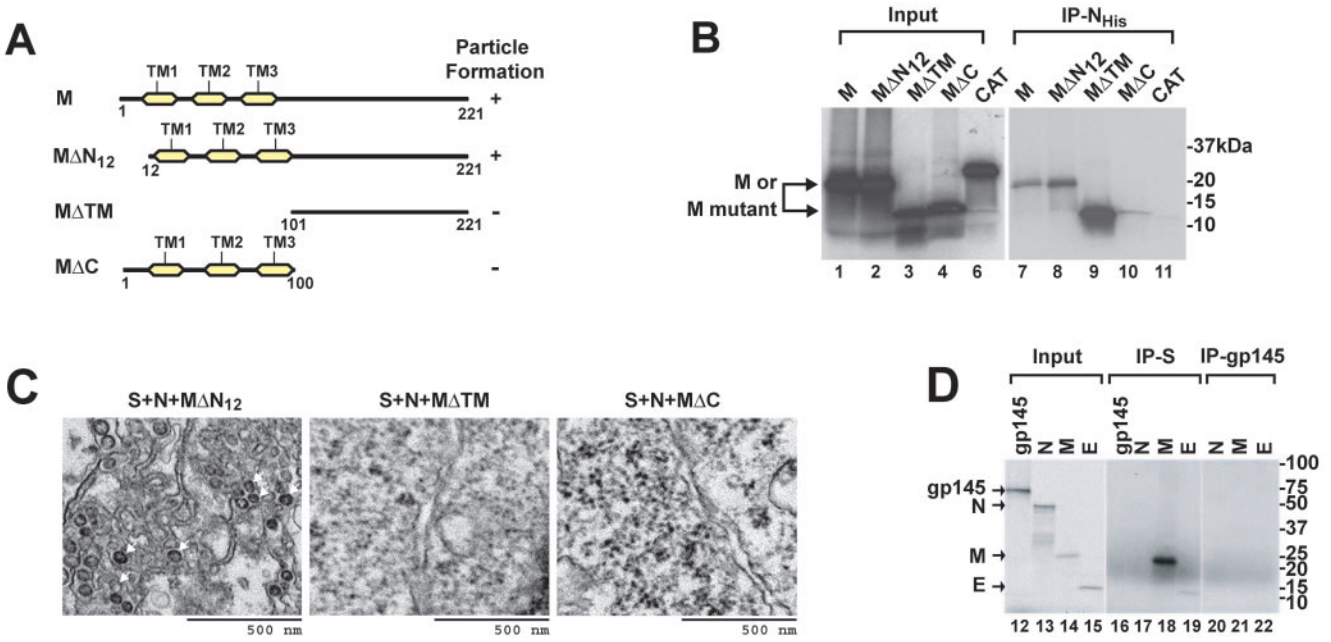


FIG. 5. Expression and interaction of M and N gene products in vitro and model of the interactions leading to the formation of SARS-CoV. (A) Schematic representation of M expression vector and mutants. The ability of the indicated mutants to form nucleocapsids in combination with N is shown. The diagram shows the assembly of VLPs by cotransfection of M mutants with S and N. (B) Immunoprecipitation and coassociation of in vitro translated M and indicated mutants by using recombinant His-tagged N protein. Proteins were transcribed and translated in vitro with reticulocyte lysate and immunoprecipitated by a polyclonal anti-His tag antiserum and protein G agarose. (C) Transfections and transmission EM analysis were performed as described in the legend of Fig. 1 (magnification, ×20,000). (D) Coassociation of in vitro translated M and E, but not N or a mutant HIV envelope protein gp145 (2), with S. Proteins were transcribed and translated in vitro with reticulocyte lysate (left) and immunoprecipitated by a human monoclonal antibody to SARS S (middle) or to HIV Env (right) and protein G agarose as described in Materials and Methods.

SARS-CoV, two of these gene products, NP and VP35, appear to give rise to the nucleocapsid, while the third, VP24, may play a catalytic role in assembly.

Previous studies with animal coronaviruses have suggested that the M protein is associated with the viral envelope and possibly associates with N in cells infected with either MHV (34) or porcine TGEV (7, 10, 19, 27). Because the sequence of the M gene product in SARS-CoV is unrelated to that in MHV or TGEV coronaviruses (less than 40% amino acid similarity), it was not clear whether analogous interactions might be found in SARS-CoV. For example, another study suggested that M and E were sufficient for particle formation in MHV (34). In the case of TGEV, N may interact with the COOH-terminal domain of M (10), but its mechanism of assembly is not necessarily the same as that in SARS-CoV in terms of its molecular interactions. The M protein of TGEV extends an additional 60 amino acids in length and is almost 30% longer than the SARS M protein. Moreover, these extra amino acids form two more putative transmembrane domains, as predicted by three different programs. This may partially explain why the E protein appears more essential for TGEV and MHV VLP assembly (1, 11).

The requirement for M and N in SARS capsid formation suggests that they perform complementary functions: M is likely anchored in the endoplasmic reticulum membrane through its transmembrane domains and its COOH-terminal domain and might facilitate the nucleation of N polymers through a specific biochemical interaction (Fig. 6). While the SARS M protein interacts biochemically with N to facilitate nucleocapsid formation through its COOH-terminal domain, M also interacts with S through its $NH_2$ terminus, and so it does not appear that S binds directly to N (Fig. 5D, lane 17, and Fig. 6). In either case, these viral gene products play distinct roles in the virus life cycle: while S mediates viral attachment and entry into target cells, M apparently promotes the formation of the capsid in combination with N.

The generation of viral genome-free SARS-CoV-like particles in this study has implications for vaccine production. The morphology and subcellular location of these VLPs and SARS-CoV are strikingly similar (Fig. 3). These VLPs further show the expected buoyant density of coronaviruses. Though extracellular release of the VLPs is not efficient, it was possible to readily collect sufficient quantities of pseudoparticles from transfected cell extracts to characterize them by sedimentation gradient centrifugation. It also remains possible that the yields of the released particles can be improved by varying the ratio of these proteins or E. The generation of replication-defective VLPs from synthetic viral expression vectors provides a safer means to prepare inactive virus particles and eliminates concerns of recombination with viral genomic RNA in vaccines. At the same time, this system provides a valuable tool for research into SARS-CoV assembly. This system can be used to analyze the structure of the viral capsid, as well as the biochemical interactions required to generate viral particles. Definition of the molecular interactions required for assembly lends insight into potential inhibitors of viral replication and sug-

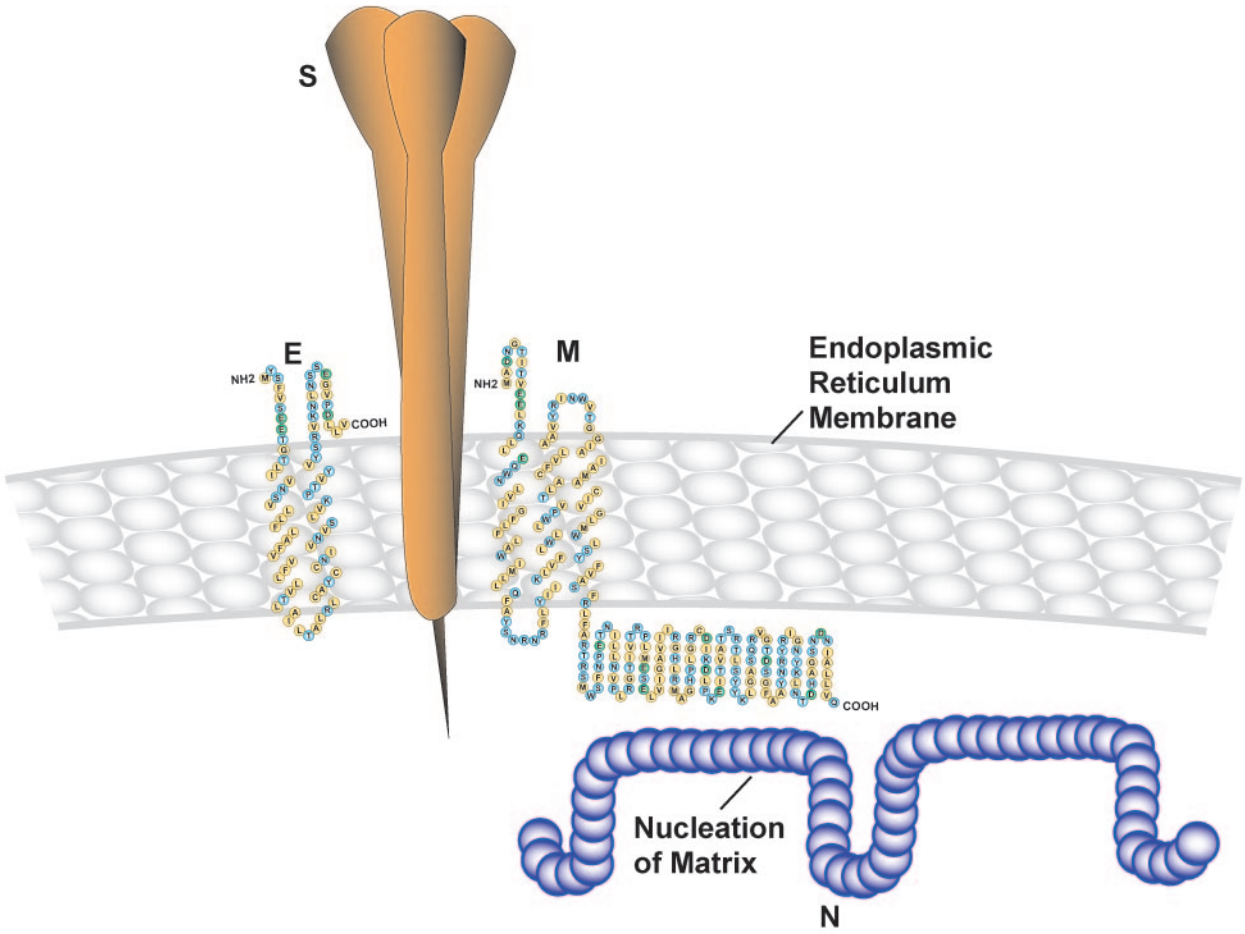


FIG. 6. Proposed schema of interactions between S, M, and N and their roles in nucleocapsid formation and viral assembly. The newly synthesized M protein is anchored in intracellular membrane through its membrane-spanning region. The COOH-terminal domain of M interacts with N to facilitate formation of nucleocapsids. In the membrane, the transmembrane domain of S may interact with M to promote viral particle budding. The E protein interacts with S independent of the S interaction with M.

gests that the COOH-terminal domain of M is a target for the development of antiviral agents. The ability to form such particles also may assist in not only the production of vaccines but also the development of diagnostic assays and antiviral drugs.

## ACKNOWLEDGMENTS

We thank Barbara Rogers at the University of Michigan for help with transmission electron microscopic analysis, William Bellini of the Centers for Disease Control for convalescent antisera to the SARS-CoV, Karen Stroud for preparing figures and artwork, Tina Suhana and Ati Tislerics for manuscript preparation, and members of the Nabel lab for helpful advice and discussion.

## REFERENCES

1. **Baudoux, P., C. Carrat, L. Besnardeau, B. Charley, and H. Laude.** 1998. Coronavirus pseudoparticles formed with recombinant M and E proteins induce alpha interferon synthesis by leukocytes. J. Virol. **72:**8636–8643.
2. **Chakrabarti, B. K., W. P. Kong, B.-Y. Wu, Z.-Y. Yang, J. Friborg, Jr., X. Ling, S. R. King, D. C. Montefiori, and G. J. Nabel.** 2002. Modifications of the human immunodeficiency virus envelope glycoprotein enhance immunogenicity for genetic immunization. J. Virol. **76:**5357–5368.
3. **Chen, C., and H. Okayama.** 1987. High-efficiency transformation of mammalian cells by plasmid DNA. Mol. Cell. Biol. **7:**2745–2752.
4. **Corse, E., and C. E. Machamer.** 2000. Infectious bronchitis virus E protein is targeted to the Golgi complex and directs release of virus-like particles. J. Virol. **74:**4319–4326.
5. **Corse, E., and C. E. Machamer.** 2003. The cytoplasmic tails of infectious bronchitis virus E and M proteins mediate their interaction. Virology **312:** 25–34.
6. **de Haan, C. A., L. Kuo, P. S. Masters, H. Vennema, and P. J. Rottier.** 1998. Coronavirus particle assembly: primary structure requirements of the membrane protein. J. Virol. **72:**6838–6850.
7. **de Haan, C. A., M. Smeets, F. Vernooij, H. Vennema, and P. J. Rottier.** 1999. Mapping of the coronavirus membrane protein domains involved in interaction with the spike protein. J. Virol. **73:**7441–7452.
8. **Delchambre, M., D. Gheysen, D. Thines, C. Thiriart, E. Jacobs, E. Verdin, M. Horth, A. Burny, and F. Bex.** 1989. The GAG precursor of simian immunodeficiency virus assembles into virus-like particles. EMBO J. **8:**2653–2660.
9. **Drosten, C., S. Gunther, W. Preiser, S. van der Werf, H. R. Brodt, S. Becker, H. Rabenau, M. Panning, L. Kolesnikova, R. A. Fouchier, A. Berger, A. M. Burguiere, J. Cinatl, M. Eickmann, N. Escriou, K. Grywna, S. Kramme, J. C. Manuguerra, S. Muller, V. Rickerts, M. Sturmer, S. Vieth, H. D. Klenk, A. D. Osterhaus, H. Schmitz, and H. W. Doerr.** 2003. Identification of a novel coronavirus in patients with severe acute respiratory syndrome. N. Engl. J. Med. **348:**1967–1976.
10. **Escors, D., J. Ortego, H. Laude, and L. Enjuanes.** 2001. The membrane M protein carboxy terminus binds to transmissible gastroenteritis coronavirus core and contributes to core stability. J. Virol. **75:**1312–1324.
11. **Fischer, F., C. F. Stegen, P. S. Masters, and W. A. Samsonoff.** 1998. Analysis of constructed E gene mutants of mouse hepatitis virus confirms a pivotal role for E protein in coronavirus assembly. J. Virol. **72:**7885–7894.
12. **Friborg, J., Jr., W. Kong, M. O. Hottiger, and G. J. Nabel.** 1999. p53 inhibition by the LANA protein of KSHV protects against cell death. Nature **402:**889–894.
13. **Gheysen, D., E. Jacobs, F. deForesta, C. Thiriart, M. Francotte, D. Thines,**

**and M. De Wilde.** 1989. Assembly and release of HIV-1 precursor Pr55gag virus-like particles from recombinant baculovirus-infected insect cells. Cell **59:**103–112.

14. **Guan, Y., B. J. Zheng, Y. Q. He, X. L. Liu, Z. X. Zhuang, C. L. Cheung, S. W. Luo, P. H. Li, L. J. Zhang, Y. J. Guan, K. M. Butt, K. L. Wong, K. W. Chan, W. Lim, K. F. Shortridge, K. Y. Yuen, J. S. Peiris, and L. L. Poon.** 2003. Isolation and characterization of viruses related to the SARS coronavirus from animals in southern China. Science **302:**276–278.
15. **Holmes, K. V.** 2001. Coronaviruses, p. 1187–1203. *In* D. M. Knipe, P. M. Howley, D. E. Griffin, M. A. Martin, R. A. Lamb, B. Roizman, and S. E. Straus (ed.), Fields virology, 4th ed. Lippincott Williams & Wilkins, Philadelphia, Pa.
16. **Huang, Y., W. Kong, and G. J. Nabel.** 2001. Human immunodeficiency virus type 1-specific immunity after genetic immunization is enhanced by modification of Gag and Pol expression. J. Virol. **75:**4947–4951.
17. **Huang, Y., L. Xu, Y. Sun, and G. J. Nabel.** 2002. The assembly of Ebola virus nucleocapsid requires virion-associated proteins 35 and 24 and posttranslational modification of nucleoprotein. Mol. Cell **10:**307–316.
18. **Ksiazek, T. G., D. Erdman, C. S. Goldsmith, S. R. Zaki, T. Peret, S. Emery, S. Tong, C. Urbani, J. A. Comer, W. Lim, P. E. Rollin, S. F. Dowell, A. E. Ling, C. D. Humphrey, W. J. Shieh, J. Guarner, C. D. Paddock, P. Rota, B. Fields, J. DeRisi, J. Y. Yang, N. Cox, J. M. Hughes, J. W. LeDuc, W. J. Bellini, and L. J. Anderson.** 2003. A novel coronavirus associated with severe acute respiratory syndrome. N. Engl. J. Med. **348:**1953–1966.
19. **Kuo, L., and P. S. Masters.** 2002. Genetic evidence for a structural interaction between the carboxy termini of the membrane and nucleocapsid proteins of mouse hepatitis virus. J. Virol. **76:**4987–4999.
20. **Lai, M. M. C., and K. V. Holmes.** 2001. *Coronaviridae*: the viruses and their replication, p. 1163–1185. *In* D. M. Knipe, P. M. Howley, D. E. Griffin, R. A. Lamb, M. A. Martin, B. Roizman, and S. E. Straus (ed.), Fields virology, 4th ed. Lippincott, Williams & Wilkins, Philadelphia, Pa.
21. **Li, W., M. J. Moore, N. Vasilieva, J. Sui, S. K. Wong, M. A. Berne, M. Somasundaran, J. L. Sullivan, K. Luzuriaga, T. C. Greenough, H. Choe, and M. Farzan.** 2003. Angiotensin-converting enzyme 2 is a functional receptor for the SARS coronavirus. Nature **426:**450–454.
22. **Locker, J. K., J. K. Rose, M. C. Horzinek, and P. J. Rottier.** 1992. Membrane assembly of the triple-spanning coronavirus M protein. Individual transmembrane domains show preferred orientation. J. Biol. Chem. **267:**21911–21918.
23. **Luo, L., Y. Li, S. Dales, and C. Y. Kang.** 1994. Mapping of functional domains for HIV-2 gag assembly into virus-like particles. Virology **205:**496–502.
24. **Macnaughton, M. R., and H. A. Davies.** 1980. Two particle types of avian infectious bronchitis virus. J. Gen. Virol. **47:**365–372.
25. **Manthorpe, M., F. Cornefert-Jensen, J. Hartikka, J. Felgner, A. Rundell, M. Margalith, and V. Dwarki.** 1993. Gene therapy by intramuscular injection of plasmid DNA: studies on firefly luciferase gene expression in mice. Hum. Gene Ther. **4:**419–431.
26. **Marra, M. A., S. J. Jones, C. R. Astell, R. A. Holt, A. Brooks-Wilson, Y. S. Butterfield, J. Khattra, J. K. Asano, S. A. Barber, S. Y. Chan, A. Cloutier, S. M. Coughlin, D. Freeman, N. Girn, O. L. Griffith, S. R. Leach, M. Mayo, H. McDonald, S. B. Montgomery, P. K. Pandoh, A. S. Petrescu, A. G. Robertson, J. E. Schein, A. Siddiqui, D. E. Smailus, J. M. Stott, G. S. Yang, F. Plummer, A. Andonov, H. Artsob, N. Bastien, K. Bernard, T. F. Booth, D. Bowness, M. Czub, M. Drebot, L. Fernando, R. Flick, M. Garbutt, M. Gray, A. Grolla, S. Jones, H. Feldmann, A. Meyers, A. Kabani, Y. Li, S. Normand, U. Stroher, G. A. Tipples, S. Tyler, R. Vogrig, D. Ward, B. Watson, R. C. Brunham, M. Krajden, M. Petric, D. M. Skowronski, C. Upton, and R. L. Roper.** 2003. The genome sequence of the SARS-associated coronavirus. Science **300:**1399–1404.
27. **Narayanan, K., A. Maeda, J. Maeda, and S. Makino.** 2000. Characterization of the coronavirus M protein and nucleocapsid interaction in infected cells. J. Virol. **74:**8127–8134.
28. **Poutanen, S. M., D. E. Low, B. Henry, S. Finkelstein, D. Rose, K. Green, R. Tellier, R. Draker, D. Adachi, M. Ayers, A. K. Chan, D. M. Skowronski, I. Salit, A. E. Simor, A. S. Slutsky, P. W. Doyle, M. Krajden, M. Petric, R. C. Brunham, and A. J. McGeer.** 2003. Identification of severe acute respiratory syndrome in Canada. N. Engl. J. Med. **348:**1995–2005.
29. **Rammensee, H. G., and M. J. Bevan.** 1984. Evidence from in vitro studies that tolerance to self antigens is MHC-restricted. Nature **308:**741–744.
30. **Rota, P. A., M. S. Oberste, S. S. Monroe, W. A. Nix, R. Campagnoli, J. P. Icenogle, S. Penaranda, B. Bankamp, K. Maher, M. H. Chen, S. Tong, A. Tamin, L. Lowe, M. Frace, J. L. DeRisi, Q. Chen, D. Wang, D. D. Erdman, T. C. Peret, C. Burns, T. G. Ksiazek, P. E. Rollin, A. Sanchez, S. Liffick, B. Holloway, J. Limor, K. McCaustland, M. Olsen-Rasmussen, R. Fouchier, S. Gunther, A. D. Osterhaus, C. Drosten, M. A. Pallansch, L. J. Anderson, and W. J. Bellini.** 2003. Characterization of a novel coronavirus associated with severe acute respiratory syndrome. Science **300:**1394–1399.
31. **Ruan, Y. J., C. L. Wei, A. L. Ee, V. B. Vega, H. Thoreau, S. T. Su, J. M. Chia, P. Ng, K. P. Chiu, L. Lim, T. Zhang, C. K. Peng, E. O. Lin, N. M. Lee, S. L. Yee, L. F. Ng, R. E. Chee, L. W. Stanton, P. M. Long, and E. T. Liu.** 2003. Comparative full-length genome sequence analysis of 14 SARS coronavirus isolates and common mutations associated with putative origins of infection. Lancet **361:**1779–1785.
32. **Siddell, S. G.** 1995. The small-membrane protein, p. 181–189. *In* S. G. Siddell (ed.), The *Coronaviridae*. Plenum Press, New York, N.Y.
33. **Smith, A. J., N. Srinivasakumar, M. L. Hammarskjold, and D. Rekosh.** 1993. Requirements for incorporation of Pr160gag-pol from human immunodeficiency virus type 1 into virus-like particles. J. Virol. **67:**2266–2275.
34. **Vennema, H., G. J. Godeke, J. W. Rossen, W. F. Voorhout, M. C. Horzinek, D. J. Opstelten, and P. J. Rottier.** 1996. Nucleocapsid-independent assembly of coronavirus-like particles by co-expression of viral envelope protein genes. EMBO J. **15:**2020–2028.
35. **Wills, J. W., R. C. Craven, and J. A. Achacoso.** 1989. Creation and expression of myristylated forms of Rous sarcoma virus Gag protein in mammalian cells. J. Virol. **63:**4331–4343.